15TH IEA HEAT PUMP CONFERENCE
MAY 26–29, 2026 | HOFBURG
VIENNA 2026
DECARBONISATION THROUGH INNOVATION

Thermodynamic performance of booster heat pumps using low-GWP zeotropic mixtures

Tingting Zhu[a*], Jierong Liang[b*], Yanjun Du[c], Jan Eric Thorsen[d], Jonas Kjær Jensen[e]

[a] Department of Thermal and Fluid Engineering, University of Twente, 7522NB Enschede, The Netherlands
[b] Helmholtz-Zentrum Dresden-Rossendorf (HZDR), Bautzner Landstraße 400, 01328 Dresden, Germany
[c] Beijing Key Laboratory of Heat Transfer and Energy Conversion, Beijing University of Technology, Beijing, 100124, China
[d] Danfoss A/S, Nordborg, Denmark
[e] Department of Civil and Mechanical Engineering, Technical University of Denmark, 2800 Kgs, Lyngby, Denmark

Abstract

Booster heat pumps (BHPs) are used in ultra-low-temperature district heating systems to locally raise the temperature for domestic hot water production. The efficiency and environmental performance of BHPs are therefore critical for next-generation district heating networks. However, no clear consensus has yet been reached on the most suitable refrigerants for these systems. Earlier studies have shown that low-GWP refrigerant mixtures can theoretically improve the coefficient of performance compared with conventional fluids such as R134a. In this study, we investigate how using zeotropic mixtures influences the thermal behavior of a BHP. The zeotropic mixture R444A and R456A were examined to determine whether their temperature glide could provide a better match between the water and refrigerant temperature profiles. The analysis was carried out using a numerical system model validated against experimental data for the zeotropic mixture R32/R1234yf. The results indicate that BHP cycles employing refrigerant mixtures can enhance both COP and exergetic efficiency when an appropriate glide match is achieved between the refrigerant and the heat source/sink during DHW preparation. Under the studied conditions, using R456A in a booster heat pump yields a COP of 5.1 and an exergetic efficiency of 47.4%.

Keywords: Booster heat pump; Zeotropic mixture; Temperature glide; Low GWP; COP

1. Introduction

The development of fourth and fifth-generation district heating (4GDH/5GDH) networks characterized by low supply temperatures and improved thermal integration, creates new opportunities for highly efficient heat pump operation. These low-temperature networks increase the relevance of refrigerants and system designs that can maintain high performance under reduced temperature lifts. Using zeotropic mixtures can achieve significant efficiency improvements (10–30%), strengthening the business case for heat pumps in residential construction. The use of zeotropic refrigerants is a promising strategy for improving the efficiency of heat pumps. Unlike pure refrigerants, which have a constant phase transition temperature, zeotropic mixtures exhibit a temperature glide, allowing the temperature of the refrigerant to more closely match that of the heat source and heat sink. This improves thermodynamic performance of the cycle and increases system efficiency [1,2]. Controlled composition changes during the phase transition allow heat pumps with zeotropic mixtures to operate within a wider temperature range, with a higher COP and lower environmental impact.

A promising strategy to improve heat pump (HP) efficiency is the use of zeotropic mixtures as working fluids. Unlike pure refrigerants with constant phase-change temperatures, zeotropic mixtures exhibit a

*1st Corresponding author. Tel.: +031 53 489 8823 *E-mail address:* t.zhu@utwente.nl (Dr. T. Zhu)
* 2nd Corresponding author. *E-mail address:* j.liang@hzdr.de (Dr. J. Liang)

temperature glide that enables closer matching between the heat source and working fluid temperature profiles. This characteristic reduces thermal irreversibility, enhances heat transfer, and improves overall system performance. Through controlled composition shifts during phase change, HPs using zeotropic mixtures can operate over broader temperature ranges, achieving higher COP and lower environmental impact [3]. By carefully selecting and tailoring these mixtures, HPs can deliver greater efficiency while reducing greenhouse gas emissions, offering a sustainable and adaptable solution for future heating and cooling applications.

Several studies have demonstrated these advantages across different applications. A Canadian case study [4] on residential HPs reported that an R32/R744 (80/20%) mixture increased heating capacity by up to 30% and COP by 8.5% compared with pure R32, with lower GWP and minimal system modifications. A feasibility study [5] on HP water heaters identified R1233zd(E)/R1270 (16/84%) as the most efficient substitute for R22 and R134a. Further works by Uddin et al. [6], Dai et al. [7], Venzik et al. [8], and others confirmed that R32-based, CO_2-based, and hydrocarbon mixtures can yield low-GWP alternatives with enhanced efficiency and improved TG matching, provided that system design minimizes pressure drops in heat exchangers. Additionally, studies on booster HPs for ultra-low-temperature district heating [2] found that R1234yf/R32 (80/20% and 90/10%) mixtures achieved up to 58% higher heating capacity and greater COP than R134a, further supporting the potential of zeotropic mixtures in advanced HP configurations. Zühlsdorf et al. [1] evaluated a booster heat pump integrated with an ultra-low-temperature district heating system for domestic hot water production. Among 18 pure fluids and zeotropic mixtures tested, R1270/R600 (50/50%) and R1234yf/R1233zd(E) (50/50%) showed superior thermodynamic performance, confirming the economic feasibility of using zeotropic mixtures despite slightly higher investment costs.

Two key insights emerge from the literature: (1) refrigerant mixtures can be customized to balance thermodynamic performance and environmental objectives, and (2) the “optimal” mixture depends strongly on boundary conditions such as source temperature, temperature glide, COP, exergy efficiency, and refrigerant composition [4,6,7,9–12]. While temperature glide enables better temperature matching and improved thermodynamic performance, it also requires careful consideration of heat and mass transfer characteristics in heat exchanger design [13]. Liang et al. [14] developed a thermal network model which is an efficient approach to conduct such optimization study. Therefore, optimizing zeotropic mixture refrigerant implementation system control and configuration is essential to ensure efficient operation across different applications, especially in the districting heating system serve either as central heat pump or as local booster heat pumps. Our research evaluates the thermodynamic characteristics of zeotropic refrigerant mixtures together with their real-world performance in residential booster heat pump systems [15]. This approach allows us to understand how temperature glide influences booster heat pump performance using a well-validated simulation model, and provides a solid reference for the application of zeotropic mixtures in such systems.

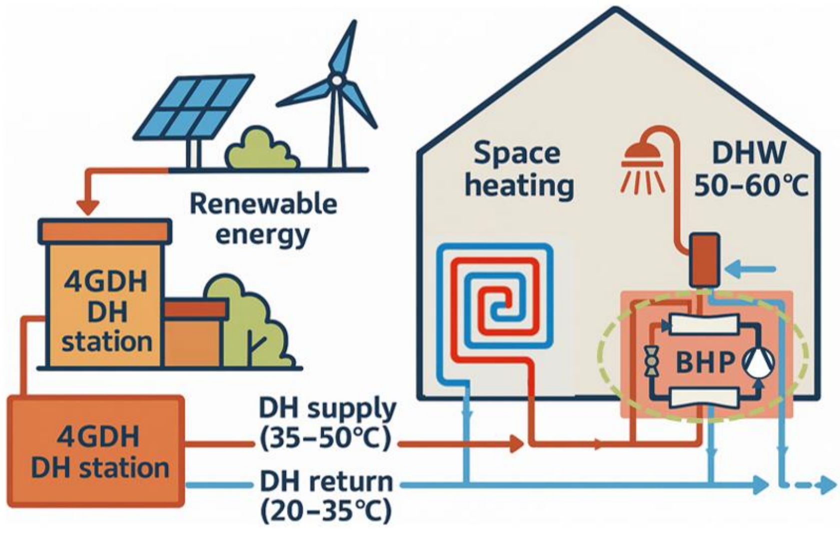

Figure 1. Booster heat pump with zeotropic mixture in 4th/5th ultra-low temperature district heating system [2].

2. Methodology

2.1. Zeotropic mixtures

Figure 2 compares the contribution of a zeotropic mixture refrigerant to the improvement of exergy efficiency relative to a pure fluid. Zeotropic mixtures exhibit a temperature glide, allowing the refrigerant temperature to more closely follow that of the heat source and heat sink. As shown in the figure, the temperature glide within the two-phase region of the zeotropic mixture enables a better thermal match between the refrigerant flow and the secondary loop fluid (water). Compared to pure fluids, this improved temperature matching reduces exergy losses.

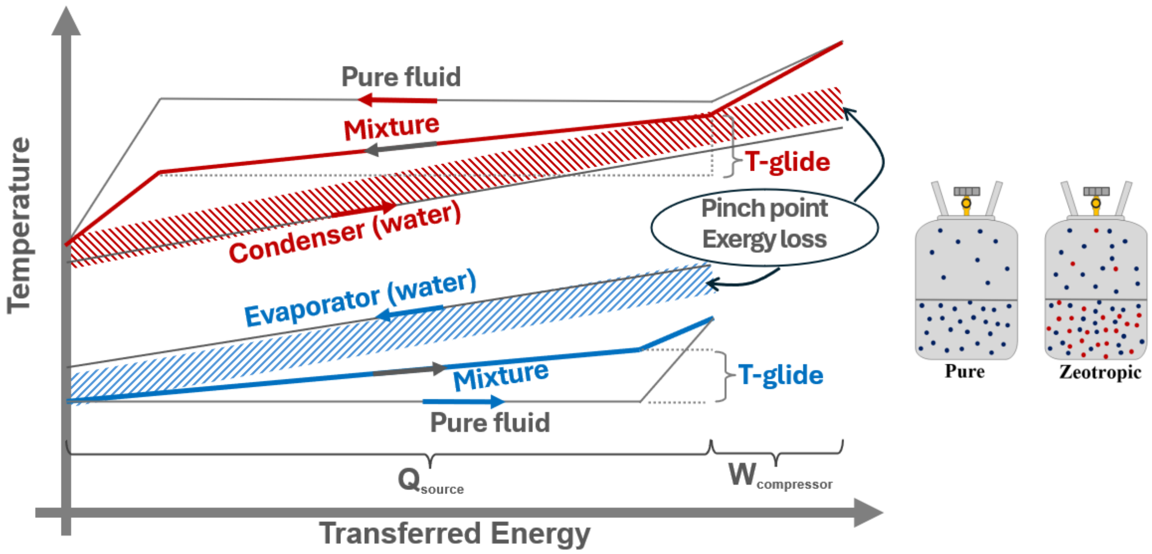

Figure 2. Temperature profile comparison between pure fluid and zeotropic mixture refrigerant in a heat pump system.

In this study, a MATLAB-based numerical model was developed to evaluate the influence of using refrigerant mixtures on the thermal performance of the BHP system. Previous studies have identified R456A and R444A as non-flammable refrigerants suitable for direct R134a replacement in air conditioning systems, with considerable potential for improving system performance [16,17]. The investigated mixtures include the zeotropic refrigerants R444A and R456A. The objective is to assess the temperature regulation profile for zeotropic mixture-based BHP systems and to support their potential application in $4^{th}/5^{th}$ generation district heating networks.

2.2. Development of numerical model

The booster heat-pump system was developed using a steady-state vapor-compression cycle coupled with a UA–LMTD heat-exchanger formulation. The computational framework was implemented in MATLAB/Python, and all refrigerant thermophysical properties were obtained from REFPROP 10.0. The cycle consists of the four standard components: evaporator, compressor, condenser, and expansion valve (as illustrated in Fig. 3).

The model accepts as inputs the external fluid boundary conditions (source and sink inlet temperatures and mass flow rates), thermophysical properties of the secondary/water fluids, superheat and subcooling, compressor isentropic efficiency, and the overall heat-transfer coefficients for the evaporator and condenser. For a given operating condition, the solver iteratively determines the refrigerant evaporating and condensing temperatures.

An initial pair of guesses for the evaporating temperature T_{evap} and condensing temperature T_{cond} is supplied to the solver. These temperatures are used to evaluate the corresponding suction and discharge pressures and the thermodynamic state points of the refrigerant (h_1, h_2, h_3, h_4), as computed by REFPROP. The refrigerant mass flow rate is then independently estimated for each heat exchanger using the UA–LMTD method, which relates the heat-transfer rate to the temperature driving forces imposed by the external fluid streams. The solver updates T_{evap} and T_{cond} until the refrigerant mass flow rates predicted by the evaporator and condenser converge within a prescribed tolerance, ensuring overall cycle energy balance.

The model yields a comprehensive set of thermodynamic and performance indicators, including the outlet temperatures of the source and sink streams (T_{source_out}, T_{sink_out}), refrigerant suction and discharge pressures, heating and cooling capacities (Q_e, Q_c), and the compressor power consumption. From these quantities, the heating and cooling coefficients of performance are subsequently evaluated. By employing the UA–LMTD formulation, the model establishes a direct and consistent coupling between refrigerant-side thermodynamics and heat-exchanger performance.

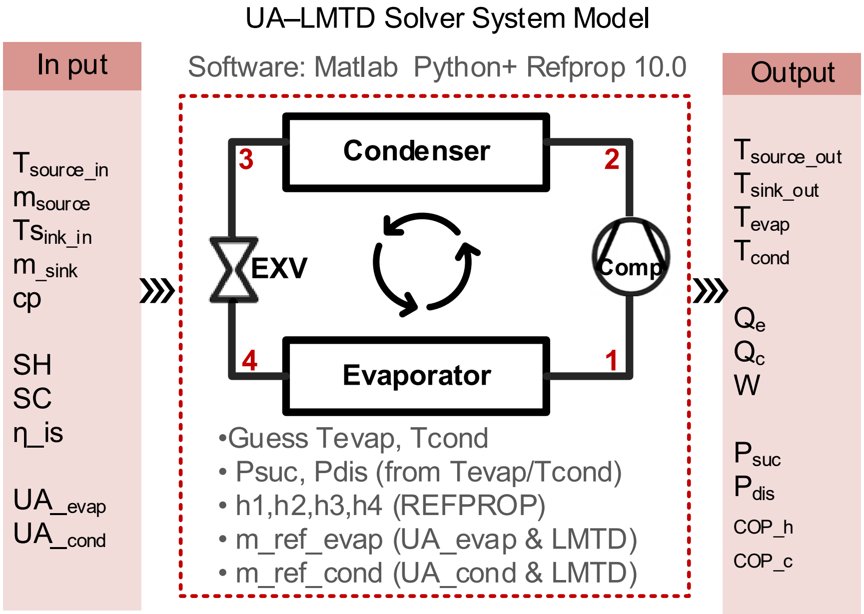

Figure 3. Flow chart of the zeotropic mixture heat pump simulation model.

2.3. Boundary conditions and assumptions

All simulations were performed under steady-state conditions. The source and sink water loops were treated as single-phase flows with constant specific heat, and heat losses to the environment were neglected. Fixed superheat and subcooling were applied, pressure drops were ignored, and the expansion process was assumed isenthalpic. The evaporator and condenser were modeled using constant UA values, and the compressor operated at a fixed isentropic efficiency. The overall heat transfer coefficient (UA) value used in the simulations was determined based on the characteristics of the investigated heat exchanger and calibrated using experimental data obtained with R1234yf/R32 (8/2) under identical operating conditions. The resulting UA values therefore reflect the fixed geometry of the heat exchanger and the heat transfer performance on the secondary fluid side, which remain unchanged for all working fluids considered in this study. The numerical inputs used in the model are summarized in Table 1.

Table 1. Numerical inputs used in the simulation

Parameter	Value	Parameter	Value
Source-side inlet temperature	40 °C	Superheat (SH)	9 K
Source-side mass flow rate	0.208 $kg \cdot s^{-1}$	Subcooling (SC)	8 K
Sink-side inlet temperature	40 °C	Compressor isentropic efficiency	70 %
Sink-side mass flow rate	0.218 $kg \cdot s^{-1}$	Evaporator UA	2300 $W \cdot K^{-1}$
Specific heat of water	4.180 $kJ \cdot kg^{-1} \cdot K^{-1}$	Condenser UA	2400 $W \cdot K^{-1}$

2.4. Equations

Utilizing REFPROP version 10.0 [18], refrigerant properties are calculated based on the input data of the studied condition as well as experimental data used for simulation model validation. The COP of BHP is calculated according to:

$$\mathrm{COP} = \frac{\dot{Q}_h}{\dot{W}_{comp}} \quad (1)$$

where $\dot{W}_{comp}$[kW] is the power consumption of the compressor and $\dot{Q}_{\mathrm{h}}$ is the heating capacity [kW].

Heating capacities can be derived from both water side and refrigerant side data:

$$\dot{Q}_{\mathrm{w,h}} = c_{\mathrm{p}}\dot{m}_{\mathrm{w,c}}(t_{\mathrm{w,c,o}} - t_{\mathrm{w,c,i}}) \tag{2}$$

$$\dot{Q}_{\mathrm{r,h}} = \dot{m}_{\mathrm{r}}(h_{\mathrm{r,c,o}} - h_{\mathrm{r,c,i}}) \tag{3}$$

with c_{p} [kJ/(kg·K)] the specific heat capacity of water, $\dot{m}_{\mathrm{w,c}}$ [kg/s] the water mass flow rate in the condenser, $t_{\mathrm{w,c,i}}$ [°C] the water inlet temperature of the condenser, and $t_{\mathrm{w,c,o}}$ [°C] the water outlet temperature of the condenser. Alternatively, $\dot{m}_{\mathrm{r}}$ [kg/s] represents the mass flow rate of the refrigerant, while $h_{\mathrm{r,c,o}}$ [kJ/(kg)] and $h_{\mathrm{r,c,i}}$ [kJ/(kg)] represents the enthalpy of the refrigerant at the condenser outlet and inlet respectively. $\dot{Q}_{\mathrm{w,h}}$ is used as the heating capacity for the COP calculation.

The isentropic compressor power is calculated according to:

$$\dot{W}_{\mathrm{is}} = \dot{m}_r(h_{\mathrm{comp,i}} - h_{\mathrm{comp,o,is}}) \tag{9}$$

with $h_{\mathrm{comp,i}}$ [kJ/kg] the enthalpy at the compressor inlet and $h_{\mathrm{comp,o,is}}$ [kJ/kg] the enthalpy at the compressor outlet based on isentropic compression.

Based on the exergy flow definition in [19], exergy enters the system from both the ULTDH central supply and the local booster, while exergy leaves through the thermal demands. In this study, the exergy demand for DHW preparation is the only exergy outflow considered, and space heating is omitted [2]. Exergy consumption includes the electrical input to the booster and the exergy supplied by the district heating network [20]. The exergetic efficiency for DHW preparation is defined as follows:

$$\eta_{\mathrm{Ex,DHW}} = \frac{\dot{Ex}_{\mathrm{DHW}}}{\dot{Ex}_{\mathrm{DH}}+\dot{Ex}_{\mathrm{BHP}}} = \frac{\dot{m}_{\mathrm{sink}}(\dot{ex}_{\mathrm{w,c,o}}-\dot{ex}_{\mathrm{DH,ret}})}{(\dot{m}_{\mathrm{sink}}+\dot{m}_{\mathrm{source}})(\dot{ex}_{\mathrm{DH,i}}-\dot{ex}_{\mathrm{DH,ret}})+\dot{W}_{\mathrm{comp}}} \tag{10}$$

where $\dot{Ex}_{\mathrm{DHW}}$ [kW] is the exergy flow of DHW demand, $\dot{Ex}_{\mathrm{DH}}$ [kW] is the exergy flow from the DH network, $\dot{Ex}_{\mathrm{BHP}}$ [kW] is the exergy flow of electricity used for local BHP, $\dot{m}_{\mathrm{sink}}$ [kg/s] is the sink water mass flow rate, $\dot{m}_{\mathrm{source}}$ [kg/s] is the source water mass flow rate, $\dot{ex}_{\mathrm{w,c,o}}$ [kW/kg] is the exergy flux of water at the condenser outlet, where its temperature $t_{\mathrm{w,c,o}}$. $\dot{ex}_{\mathrm{DH,ret}}$ [kW/kg] is the DH return exergy flux, $\dot{ex}_{\mathrm{DH,i}}$ [kW/kg] is the DH inlet exergy flux.

Table 2. Thermophysical properties of the studied alternative low-GWP refrigerants and the reference R134a

Property	**R444A**	**R456A**	**R134A** [16]
Component composition (wt%)	R1234ze(E)/R32/R152a =83%/12%/5%	R1234ze(E)/R134a/R32 =49%/ 45%/ 6%	-
Molecular weight (kg/kmol)	~90	~101	~102
Normal boiling point (°C)	−19	−30.8	-26.09
Critical temperature (°C)	~110	~102.7	101.0
Critical pressure (MPa)	~3.4	~3.6	~4.06
GWP (AR4)	~90	~630–690	1430
ODP	0	0	0
ASHRAE safety class	A2L (mildly flammable)	A1 (non-flammable)	A1 (non-flammable)
Typical application	Low-GWP replacement for R-1234yf / R-134a	Drop-in substitute for R-134a (A/C, chillers)	Conventional (A/C, chillers)

3. Results and analysis

3.1. Simulation model validations

The developed model was validated using experimental data obtained with the zeotropic mixture R1234yf/R32 (mass fraction 8/2) under the same operating conditions described in Section 2.3. The validation dataset originates from our previous study [15], in which the experimental setup, measurement methodology, and uncertainty analysis were comprehensively documented. That work experimentally investigated the thermodynamic behavior of the R1234yf/R32 (8/2; 9/1) mixture, including temperature glide effects and heat transfer characteristics. In the present study, these experimentally established results are used to assess the predictive capability of the proposed model. Table 2 shows the difference between test results and the simulation results. The close agreement between model predictions and experimental measurements demonstrates the validity and robustness of the model for simulating zeotropic refrigerant mixtures under the investigated conditions.

Table 3. Model Validation

Parameters	Experimental result	Simulation result	Difference, abs	Difference, Δ %
Tsource_out, °C	23.7	21.8	1.9	8.01
Tsink_out, °C	59.1	56.2	2.9	4.91
m_ref, kg/s	0.093	0.090	0.003	3.22
Qe, kW	13.6	13.77	-0.17	-1.25
Qc, kW	18.1	17.34	0.76	4.19
COP_h	4.1	4.8	-0.70	17.1

3.2. Temperature profile

The thermodynamic and exergetic characteristics of the heat exchangers are examined through temperature–heat transfer (T– Q) diagrams, which offer a clear representation of the thermal interactions within the system. Figure 4 shows the T– Q diagrams for the booster heat pump operating with the zeotropic refrigerant blends R444A and R456A. The diagrams illustrate how variations in refrigerant temperature profiles in both the evaporator and condenser, under operating conditions with a district heating supply temperature of 40 °C. These temperature distributions highlight the effects of refrigerant glide and provide insight into the sources of exergy destruction within the heat exchangers.

Figure 4 compares the simulated temperature profiles of R1234yf/R32 (80%/20%), R444A, and R456A across heating loads from 0 to approximately 15–25 kW at same input parameters condition (Table 1). For the R1234yf/R32 mixture, the evaporator temperature increases modestly from about 13 °C to 20 °C as load rises from 0 to 15 kW, while the condenser temperature increases more sharply from roughly 50 °C to nearly 90 °C. This widening separation between source and refrigerant temperatures indicates increasing glide on the high-pressure side, leading to a progressively poorer match with the nearly linear heat-sink temperature profile. R444A shows the largest temperature excursions among the three fluids: the evaporator temperature spans from approximately 0 °C to 17 °C, whereas the condenser temperature rises steeply from about 60 °C to more than 130 °C at 23 kW. This rapid increase leads to significant mismatching with both the heat source and heat-sink profiles, especially above 15 kW, suggesting high discharge temperatures and reduced heat-exchanger effectiveness.

R456A exhibits the most moderate temperature behavior. The evaporator temperature increases from around 15 °C to 25 °C over the 0–15 kW load range, and the condenser temperature rises from roughly 55 °C to 85 °C. Both curves follow the heat-source and heat-sink lines more closely than in the other two cases, indicating improved temperature-profile matching and more favorable glide characteristics. The smaller deviation between refrigerant and external temperature profiles suggests more effective heat transfer and potentially higher system efficiency, means less exergy destruction. Overall, the numerical trends show that although all fluids achieve the required operating temperatures, R456A provides the most balanced temperature rise and the closest alignment with boundary conditions across the tested loads. Regulation of the heat sink or heat source flow rate may also improve temperature matching and should be explored further.

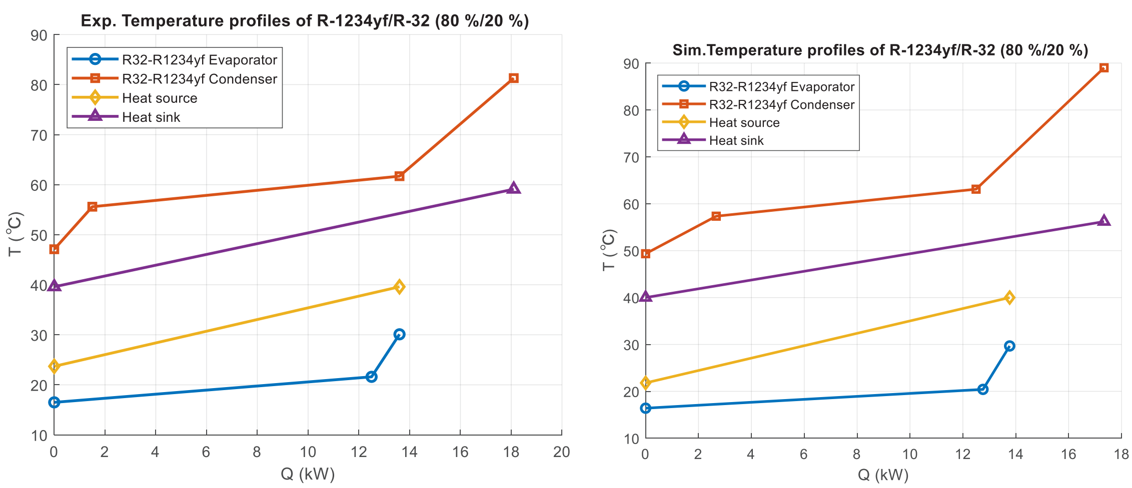

(a) (b)

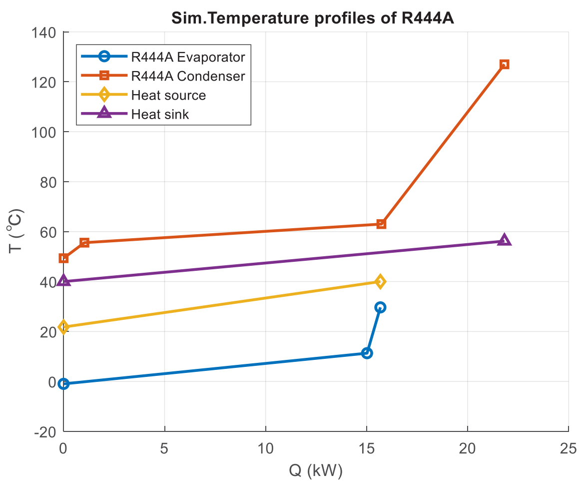

(c)

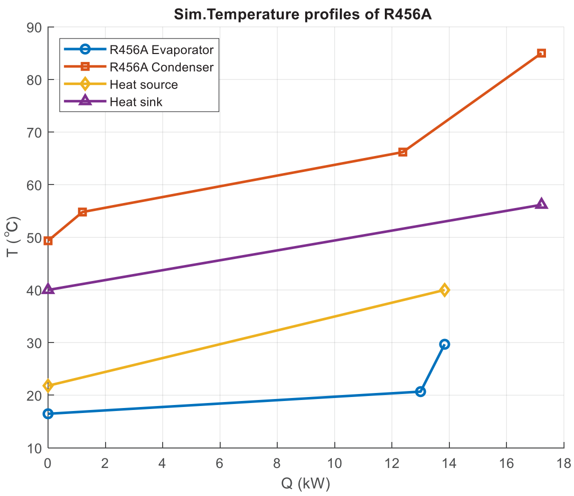

(d)

Figure 4. Temperature profiles of condenser and evaporator of BHP with a) R1234yf/R32 Exp. b) Sim., c) R444A and d) R456A.

3.3. Energy and exergy analysis

The performance analysis covers both the characteristics of the booster heat pump (BHP) operating with R456A and the boundary conditions of the district heating network. Figure 5 presents the relationships between COP, heating capacity, and exergetic efficiency of the DHW preparation system as functions of the district heating return temperature. The COP increases with DH return temperature and reaches its maximum near 21.8 °C, indicating improved heat pump performance at higher source temperatures. The heating capacity remains nearly constant across most conditions but rises noticeably at the highest temperature, suggesting enhanced heat transfer. In contrast, the exergetic efficiency decreases steadily as the return temperature increases, reflecting the reduced thermodynamic quality of the heat source. Overall, higher return temperatures improve COP and Q_c, but lead to lower exergetic efficiency, highlighting a trade-off between conventional performance and exergy-based evaluation. These trends agree with the overall behavior presented in reference [2] where results from multiple supply-temperature scenarios show an almost linear increase in both COP and $Q_c$with increasing return temperature.

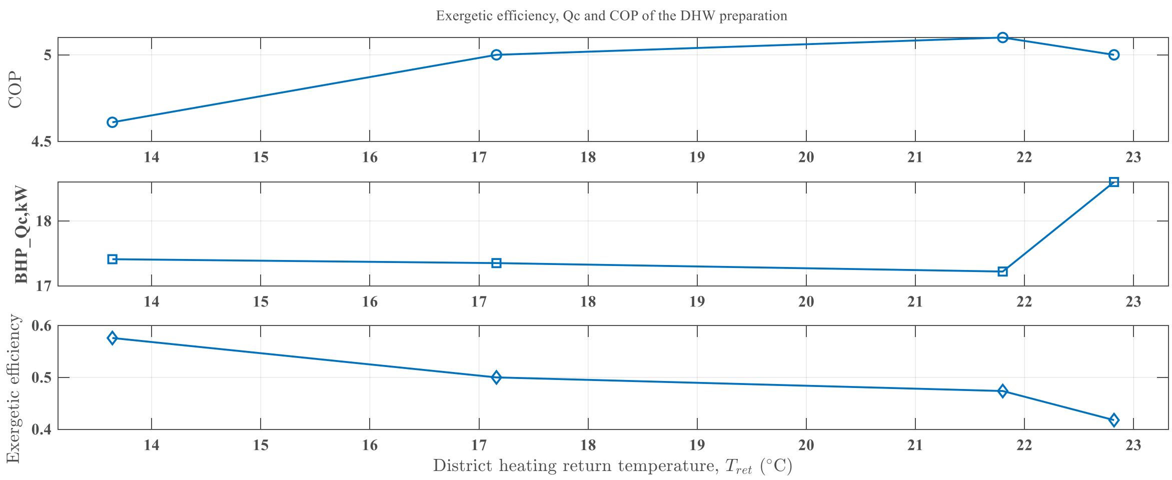

Fig. 5. Exergetic efficiency of DHW preparation system, BHP heating capacity, and COP as a function of district heating return temperature at different refrigerants.

4. Discussion

4.1. Neglect of pressure drop effects

The viscosities of the zeotropic refrigerant mixtures R1234yf/R32, R444A, and R456A vary due to differences in their component compositions and molecular interactions. In zeotropic mixtures, viscosity is not only a function of temperature and pressure but may also be influenced by composition shifts during phase change, particularly in the two-phase region. Among the mixtures considered, R444A generally exhibits higher viscosity (The higher viscosity of R444A may partly explain the increased superheating observed under identical boundary conditions, as it can reduce convective heat transfer effectiveness and promote an extended superheated vapor region.) , while R1234yf/R32 shows lower viscosity under comparable operating conditions, with R456A presenting intermediate behavior. These viscosity differences can affect pressure drop and local heat transfer characteristics in heat exchangers. In the present system-level analysis, such effects are inherently captured through the use of mixture-specific thermophysical properties, while detailed composition-dependent variations are beyond the scope of the current modeling approach.

4.2. Transient effects

The present analysis is conducted under steady-state conditions and therefore neglects transient effects such as compressor on/off cycling, load variations, and time-dependent mixture composition shifts. These effects can be particularly relevant for zeotropic mixtures, as transient operation may amplify composition redistribution and associated variations in thermophysical properties. As a result, the findings of this study should be interpreted as representative of quasi-steady operating behavior, with the comparative trends primarily reflecting steady-state thermodynamic performance. The potential influence of transient phenomena on system performance and mixture behavior is not captured within the current framework and should be considered when extending the results to dynamic operating conditions.

4.3. Constant UA and isentropic efficiency

For the zeotropic mixtures, the same UA values were applied to ensure a consistent basis for comparison in this study. Differences between pure fluids and mixtures were accounted for through their respective thermophysical properties and temperature profiles, including temperature glide during phase change. This approach allows the impact of mixture behavior on heat exchanger performance to be isolated without introducing additional uncertainty related to variable UA values.

It is noted that the assumption of a constant UA does not explicitly resolve local variations in heat transfer coefficients that may occur during the condensation/evaporation of zeotropic mixtures, particularly as a result of temperature glide and composition-dependent transport properties. However, at the system level, the use of a constant UA enables a clear assessment of overall performance trends while avoiding additional uncertainties associated with locally varying heat transfer correlations. The observed agreement between model predictions and experimental data indicates that this assumption provides a reasonable representation of the heat exchanger behavior within the investigated operating range. These results suggest that the dominant effects of zeotropic mixtures are adequately captured through their thermophysical properties and temperature profiles in the present framework. Future work will focus on relaxing this assumption by incorporating mixture-specific and locally resolved heat transfer correlations in order to further improve the physical fidelity of the model.

In the present model, a constant isentropic efficiency is assumed for the compressor for all refrigerants and refrigerant mixtures considered. This simplification does not explicitly account for potential interactions between the compressor and the working fluid, which may be particularly relevant for zeotropic mixtures due to variations in thermophysical properties, composition shift, and suction conditions. Within the scope of this study, differences in system performance are therefore mainly attributed to the thermodynamic behavior of the working fluids rather than to variations in compressor efficiency. Future work will address this limitation by incorporating refrigerant dependent compressor performance maps or experimentally derived efficiency correlations, particularly for zeotropic mixtures, to better capture interactions between compressor and zeotropic refrigerant.

4.4. Applicability of LMTD to zeotropic mixtures

The applicability of the logarithmic mean temperature difference (LMTD) method to zeotropic mixtures requires careful consideration due to the presence of temperature glide during phase change, which leads to a non-uniform temperature difference along the heat exchanger. While the LMTD approach remains useful for system-level analyses and comparative studies, it does not fully capture local thermal variations associated with mixture condensation. In the present work, the method is therefore applied in an averaged sense, providing a practical representation of the overall heat transfer behavior while ensuring consistency across different working fluids. Further investigation of segmented heat transfer behavior in both the evaporator and condenser for zeotropic mixtures is identified as a promising direction for future work.

5. Conclusions

This study evaluates the potential of the zeotropic refrigerant blends R444A and R456A for application in a booster heat pump operating within a fourth-generation district heating (4GDH) framework. A steady-state UA–LMTD system model was developed using REFPROP-based thermophysical properties, and the performance of both blends was assessed under representative boundary conditions. Owing to its larger temperature glide, R444A requires more careful regulation of the external fluid temperatures to achieve optimal performance. Under the fixed flow rate and DHW outlet temperature imposed in this study, the advantages typically associated with R444A's glide were partially diminished. In contrast, the results show that R456A can deliver competitive heating capacities and coefficients of performance while maintaining temperature lifts compatible with 4GDH supply levels. Its moderate discharge temperatures and favorable thermodynamic behavior further support its suitability as a low-GWP replacement for conventional refrigerants. The zeotropic nature of both blends offers potential benefits for heat-transfer matching in the evaporator and condenser; however, it also underscores the need for appropriate control strategies to fully exploit glide-related performance gains. Overall, the findings indicate that R456A is a promising candidate for high-efficiency booster heat pumps in next-generation district heating networks. Under the studied conditions, its COP reaches 5.1 and the exergetic efficiency of DHW production attains 47.4%.

6. Limitation and recommendation

The present model employs a steady-state UA–LMTD formulation with simplified representations of the evaporator and condenser. Although this approach provides rapid and stable solutions, it does not fully capture the detailed heat-transfer and refrigerant distribution phenomena occurring inside the heat exchangers. Future work could incorporate distributed or segment-by-segment heat-exchanger models to resolve phase-change behavior, local temperature profiles, and pressure drops more accurately. Another limitation is the assumption of steady-state operation. In practice, heat-pump systems exhibit significant transient behavior, particularly when using zeotropic mixture refrigerant. Including dynamic modeling of refrigerant inventory, mixture composition shift, and start-up or load-change behavior would substantially improve the predictive capability of the model. Such enhancements would also support advanced control strategies and facilitate more realistic system-level analyses. Overall, extending the model to include detailed heat-exchanger characterization and transient refrigerant-mixture behavior represents a valuable direction for future research.

Acknowledgements

The research leading to these results has received funding from the European Union's Horizon 2020 research and innovation program under the Marie Sklodowska-Curie grant agreement no. 713683 (H. C. Ørsted Postdoc project HPMixPerform: Performance optimization of heat pumps using zeotropic mixtures as working fluid). We gratefully acknowledge the 4TU.Energy for financial support for the dissemination of this research. (Energy Supply& Demand in Residential Buildings, no. UT20005769-10). The authors would also like to express their heartfelt gratitude to Jan Horne Hansen and Benny Edelsten (DTU) for their assistance with the experimental setup. The authors also gratefully acknowledge the late Prof. Brian Elmegaard (DTU), whose encouragement and vision continue to inspire this research.

References

[1] Zühlsdorf B, Meesenburg W, Ommen TS, Thorsen JE, Markussen WB, Elmegaard B. Improving the performance of booster heat pumps using zeotropic mixtures. Energy 2018;154:390–402.

[2] Zhu T, Vieren E, Liang J, Thorsen JE, De Paepe M, Lecompte S, et al. Booster heat pump with drop-in zeotropic mixtures applied in ultra-low temperature district heating system. Energy

2024;305:132292. https://doi.org/10.1016/J.ENERGY.2024.132292.
[3] Sefidgar Z, Khazaei A, Javaherian A, Mahmoudi SMS, Elmegaard B, Arabkoohsar A. Heat pumps using zeotropic mixtures for heating and cooling applications: A literature review. Appl Therm Eng 2025;276:126794. https://doi.org/10.1016/J.APPLTHERMALENG.2025.126794.
[4] Hakkaki-Fard A, Aidoun Z, Ouzzane M. Applying refrigerant mixtures with thermal glide in cold climate air-source heat pumps. Appl Therm Eng 2014;62:714–22. https://doi.org/10.1016/J.APPLTHERMALENG.2013.10.033.
[5] Ju F, Fan X, Chen Y, Zhang H, Wang T, Tang X. Performance assessment of heat pump water heaters with R1233zd(E)/HCs binary mixtures. Appl Therm Eng 2017;123:1345–1355,. https://doi.org/10.1016/j.applthermaleng.2017.05.137.
[6] Uddin K, Arakaki S, Saha BB. Thermodynamic analysis of low-GWP blends to replace R410A for residential building air conditioning applications, Environ. Sci Pollut Res 2021;28:2934–2947,. https://doi.org/10.1007/s11356-020-10656-9.
[7] Dai B, Dang C, Li M, Tian H, Ma Y. Thermodynamic performance assessment of carbon dioxide blends with low-Global Warming Potential (GWP) working fluids for a heat pump water heater. Int J Refrig 2014;56:1–14,. https://doi.org/10.1016/j.ijrefrig.2014.11.009.
[8] Venzik V, Roskosch D, Atakan B. Propene/isobutane mixtures in heat pumps: An experimental investigation. Int J Refrig 2017;76:84–96. https://doi.org/10.1016/J.IJREFRIG.2017.01.027.
[9] Wang B, Cheng Z, Shi W, Li X. Numerical study of gas injected heat pump using zeotropic R32/R1234ze(E) mixture: comparison of two type economizers. Appl Therm Eng 2018;142:410–420,. https://doi.org/10.1016/j.applthermaleng.2018.07.013.
[10] Cheng Z, Wang B, Shi W, Li X. Numerical research on R32/R1234ze(E) air source heat pump under variable mass concentration. Int J Refrig 2017;82:1–10,. https://doi.org/10.1016/j.ijrefrig.2017.06.014.
[11] Cui M, Wang B, Wei F, Shi W. Novel zeotropic refrigeration cycles for air cooling with large temperature decrease, Energ. Energy Build 2022;274. https://doi.org/10.1016/j.enbuild.2022.112450.
[12] Roskosch D, Venzik V, Schilling J, Bardow A, Atakan B. Beyond Temperature Glide: The Compressor is Key to Realizing Benefits of Zeotropic Mixtures in Heat Pumps. Energy Technol 2021;9:1–10. https://doi.org/10.1002/ente.202000955.
[13] Bao J, Zhang R, Yuan T, Zhang X, Zhang N, He G. A simultaneous approach to optimize the component and composition of zeotropic mixture for power generation systems. Energy Convers Manag 2018;165:354–362,. https://doi.org/10.1016/j.enconman.2018.03.072.
[14] Liang J, Zhu T, Sun L, Wang H, Li T. A thermal network model for hydrocarbon heat pump systems: A coupling analysis of configuration, working condition, and refrigeration distribution. Energy Convers Manag 2022;267:115908. https://doi.org/10.1016/J.ENCONMAN.2022.115908.
[15] Zhu T, Du Y, Liang J, Rohlfs W, Eric Thorsen J, Elmegaard B. Integration of booster heat pumps in ultra-low temperature district heating network: Prototype demonstration and refrigerant charge investigation. Energy Build 2023;298:113516. https://doi.org/10.1016/J.ENBUILD.2023.113516.
[16] Al-Sayyab AKS, Navarro-Esbrí J, Mota-Babiloni A. Energy, exergy, and environmental (3E) analysis of a compound ejector-heat pump with low GWP refrigerants for simultaneous data center cooling and district heating. Int J Refrig 2022;133:61–72. https://doi.org/10.1016/J.IJREFRIG.2021.09.036.
[17] Khalid Shaker Al-Sayyab A, Navarro-Esbrí J, Barragán-Cervera A, Mota-Babiloni A. Heating and cooling challenges for electric vehicles: A comprehensive experimental study. Therm Sci Eng Prog 2024;53:102687. https://doi.org/10.1016/J.TSEP.2024.102687.
[18] Lemmon EW, Bell IH, Huber ML, McLinden MO. NIST Standard Reference Database 23: Reference Fluid Thermodynamic and Transport Properties-REFPROP, Version 10.0, National Institute of Standards and Technology 2018. https://doi.org/https://doi.org/10.18434/T4/1502528.
[19] Yang X SS. Ultra-low temperature district heating system with central heat pump and local boosters for low-heat-density area: Analyses on a real case in Denmark. Energy 2018.
[20] Elmegaard B, Ommen TS, Markussen M, Iversen J. Integration of space heating and hot water supply in low temperature district heating. Energy Build 2016;124:255–64. https://doi.org/10.1016/J.ENBUILD.2015.09.003.